Available online at www.sciencedirect.com
SCIENCE DIRECT®
Journal of Nuclear Materials 346 (2005) 40–47
journal of nuclear materials
www.elsevier.com/locate/jnucmat

Radiolytic modelling of spent fuel oxidative dissolution mechanism. Calibration against UO_2 dynamic leaching experiments

J. Merino [a,*], E. Cera [a], J. Bruno [a], J. Quiñones [b], I. Casas [c], F. Clarens [c], J. Giménez [c], J. de Pablo [c], M. Rovira [c], A. Martínez-Esparza [d]

[a] *Enviros Spain, Pg. de Rubí 29-31, 08197 Valldoreix, Spain*
[b] *Ciemat, Av. Complutense 22, 28040 Madrid, Spain*
[c] *Department of Chemical Engineering, Universitat Politècnica de Catalunya, ETSEIB, Diagonal 647 H-4, 08028, Barcelona, Spain*
[d] *Enresa, C/Emilio Vargas 7, 28043 Madrid, Spain*

Abstract

Calibration and testing are inherent aspects of any modelling exercise and consequently they are key issues in developing a model for the oxidative dissolution of spent fuel. In the present work we present the outcome of the calibration process for the kinetic constants of a UO_2 oxidative dissolution mechanism developed for using in a radiolytic model. Experimental data obtained in dynamic leaching experiments of unirradiated UO_2 has been used for this purpose. The iterative calibration process has provided some insight into the detailed mechanism taking place in the alteration of UO_2, particularly the role of $^{\bullet}OH$ radicals and their interaction with the carbonate system. The results show that, although more simulations are needed for testing in different experimental systems, the calibrated oxidative dissolution mechanism could be included in radiolytic models to gain confidence in the prediction of the long-term alteration rate of the spent fuel under repository conditions.

PACS: 82.20; 82.20.P; 82.40; 82.59.G

1. Introduction

Assessing the performance of spent nuclear fuel in a potential future geological disposal system requires the understanding and quantification of the important time-dependent phenomena influencing its behaviour on a time-scale up to millions of years. Such a demanding goal requires the development and qualification of models predicting the long-term release rate of radionuclides. This is precisely the main objective of the European Spent Fuel Stability (SFS) project [1].

Different approaches can be used to model spent fuel dissolution. In particular, radiolytic models have been usually considered useful tools to represent the behaviour of the spent fuel/water interface [2], a complex redox system where oxidants and reductants are created by the radiolysis of water. Under anoxic or reducing conditions

* Corresponding author. Tel.: +34 93 583 0500; fax: +34 93 589 0091.
E-mail address: jmerino@enviros.biz (J. Merino).

0022-3115/$ - see front matter © 2005 Elsevier B.V. All rights reserved.
doi:10.1016/j.jnucmat.2005.05.019

the oxidants generated by the radiolytic process will be the main mechanism in the alteration/dissolution of the spent fuel.

However, radiolytic models have been controversial due to limited availability of relevant kinetic data, difficulty to handle heterogeneous systems, and a lack of model validation. In the context of the Spanish Nuclear Waste Management program and more widely the SFS project, we are developing a radiolytic model (to calculate the concentration of oxidants produced by radiolysis) coupled to a chemical model (for the reaction at the UO_2 surface) to assess the long-term alteration of the spent fuel under repository conditions. One of the key requirements for developing a model is its proper calibration and testing. In particular, we have calibrated the kinetic constants of the oxidative dissolution mechanism included in the model. This mechanism has been developed from empirical and semi-empirical models based on experimental data obtained in unirradiated UO_2 dynamic leaching experiments [3–6], with a new focus on integrating both the oxygen and hydrogen peroxide mediated mechanisms in the presence of carbonate.

2. Conceptual and mathematical model

The conceptual model for the UO_2 oxidative dissolution has been previously developed in the context of the long-term modelling of spent fuel alteration [7–10]. Briefly, when water will enter in contact with the fuel surface, the first process we may expect is the radiolysis of water. Water radiolysis will generate reductants and oxidants and we may expect local oxidising conditions. Because of these local conditions, the surface of the fuel will oxidise. The oxidation of the matrix and the attachment of aqueous ligands able to form strong complexes with its major component will favour the dissolution of the matrix. In the present work we have applied this oxidative dissolution model to unirradiated UO_2 dynamic leaching experiments, where only the oxidation of the UO_2 by the available oxidants (O_2 and H_2O_2) and the matrix dissolution are accounted for. On the other hand, precipitation of pure or mixed secondary solid phases would be expected if solubility limits are reached, in such case precipitation according to equilibrium should be approached [7]. In the following paragraphs we describe with more detail all the processes with the related mechanisms and kinetic constants included in the model.

2.1. Oxygen mediated oxidation

Different mechanisms are proposed in the literature to explain the oxygen mediated oxidation of the UO_2 matrix [4,6,11,12]. Most of them agree that surface oxidation occurs via a mechanism of electron transfer with the oxygen molecule adsorbed onto the surface of the matrix. Based on the proposed mechanisms but due to the limitations of the code, this molecular process is written by means of macroscopic elemental reactions as follows:

$$>UO_2 + O_2 \Rightarrow >UO_2 - O_2 \quad kO_2 \tag{1}$$

$$>UO_2 - O_2 + >UO_2 \Rightarrow 2{>}UO_3 \quad \text{Fast} \tag{2}$$

where $>UO_2$ represents a reactive surface site, $>UO_2 - O_2$ represents a site where a full oxygen molecule is sorbed and $>UO_3$ represents a fully oxidised surface site. The rate determining step will be the adsorption of the oxygen molecule to the co-ordination site (Eq. (1)). The rate constant of Eq. (2) will be an arbitrary value much higher than the rate constant of the first reaction, kO_2, which has been derived from the oxidative dissolution mechanism for unirradiated UO_2 proposed by de Pablo and co-workers ([6,13]), with the following reaction accounting for the oxidation of the matrix:

$$>UO_2 + 1/2O_2 \Longleftrightarrow >UO_3 \tag{3}$$

A kinetic constant for Eq. (3) was obtained by these authors by a fitting process taking into account a total density of surface sites of $10^{-6}\,\mathrm{mol\,m^{-2}}$, giving a value of $0.7\,\mathrm{M^{-1}\,s^{-1}}$ at 25 °C [11]. The kinetic constant for our mechanism, kO_2 (Eq. (1)), has been recalculated based on recent experimental data for the density of surface sites, $2.74\times10^{-4}\,\mathrm{mol\,m^{-2}}$ [14], and by developing our mechanism in agreement with the one of de Pablo et al. [4], obtaining a value of $kO_2 = 0.0013\,\mathrm{M^{-1}\,s^{-1}}$.

2.2. Hydrogen peroxide mediated oxidation

There are several hypotheses of the processes and mechanisms taking place during hydrogen peroxide oxidation. However, most of the authors agree that hydrogen peroxide oxidation occurs by radical formation with very high oxidation potentials, and with the radical hydroxyl ($^{\bullet}OH$) as one of the main species generated in this process [15–17]. In addition, H_2O_2 auto-decomposition is also known to be catalysed on oxide surfaces containing mixed oxidation states [18]. When hydrogen peroxide concentration ranges $10^{-4}\ \mathrm{M} < [H_2O_2] < 10^{-2}\ \mathrm{M}$, the oxidative dissolution and hydrogen peroxide decomposition should occur simultaneously [12]. On the other hand, most of the authors also highlight that bicarbonate may act as scavenger of the $^{\bullet}OH$ to form the radical $^{\bullet}CO_3^-$ [16]. The radical carbonate has a lower oxidation potential than the radical hydroxyl, and therefore this species is less reactive than its precursor. Experiments carried out with non irradiated UO_2 with an initial H_2O_2 concentration, and with and without carbonates in the system respectively [19], gave a lower dissolution

rate for uranium and a higher rate of consumption of hydrogen peroxide when carbonate was present in the system. The authors attributed this behaviour to a radical scavenging effect. Dissolution tests performed with spent nuclear fuel at several carbonate concentrations [20] showed different steady state concentrations of hydrogen peroxide depending on the solution composition, and more specifically on the bicarbonate content. In fact, steady state concentrations decreased when increasing the carbonate content, confirming once again the effect of this compound acting as a radical scavenger.

The mechanism proposed by Ekeroth and Jonsson [21] for the reaction between UO_2 and H_2O_2 is based on a slow one-electron transfer step accounting for the oxidation of UO_2 by $^{\cdot}OH$, with a primary step analogous to the Fenton reaction. Most of the authors agree in similar reaction sequences for the oxidation of metallic oxides by H_2O_2 based on Fenton, Fenton-like or Haber Weiss-like mechanisms [16,22].

The proposed mechanism for the H_2O_2 mediated UO_2 matrix oxidation is quite similar to the one proposed by the other authors but avoiding the formation of a U(V) surface species as intermediate. Therefore, auto-decomposition catalysed by the uranium oxide is considered in a simplified form. In such case, the mechanism proposed for the oxidation of the spent fuel matrix by hydrogen peroxide is

$$>UO_2 + H_2O_2 \Rightarrow >UO_2 + 2{\cdot}OH \quad kH_2O_2 \tag{4}$$

$$>UO_2 + {\cdot}OH \Rightarrow >UO_2OH \quad kOH \tag{5}$$

$$>UO_2OH + {\cdot}OH \Rightarrow >UO_3 + H_2O \quad \text{Fast} \tag{6}$$

The overall mechanism accounts for the general oxidation reaction by H_2O_2, that is:

$$>UO_2 + H_2O_2 \Rightarrow >UO_3 + H_2O \tag{7}$$

The kinetic constant associated to the first mechanistic reaction (Eq. (4)), that is kH_2O_2, was calibrated by using the data generated from the dissolution of non irradiated UO_2 at different hydrogen peroxide concentrations in a flow-through system [5]. The results of this calibration are presented in Section 3.2, and the resulting kinetic constant is 2.2 $M^{-1}s^{-1}$.

The constant associated to the second reaction (Eq. (5)), was derived from the work of Ekeroth and Jonsson [21]. The authors report a second order rate constant for the oxidation of UO_2 by the radical hydroxyl of 0.428 m/min (derived from the slope between the pseudo-first order kinetic constant in min^{-1} and the surface to volume ratio, m^{-1}). Thus, recalculating this rate constant we obtained $kOH = 2.6 \times 10^4$ $M^{-1}s^{-1}$. This value is the one used for Eq. (5). Once the intermediate species $>UO_2OH$ is formed, another radical oxidises this intermediate to give a U(VI) species and water. This process will be faster than the previous one. The rate limiting step will be the decomposition of H_2O_2, as this reaction has the lowest kinetic constant.

The proposed mechanism is a simplified form of the overall oxidation process by H_2O_2. This approach has the advantage of involving the $^{\cdot}OH$ radicals, and this will be a key point when calibrating the model in the presence of bicarbonate, as will be shown later on.

2.3. Matrix dissolution

The kinetic constants associated to the dissolution processes once the surface sites are oxidised have also been derived from the oxidation/dissolution mechanisms proposed by de Pablo and co-workers [5,11]. Their mechanisms are based on two dissolution steps:

- Surface co-ordination of U(VI) by the aqueous ligands (H^+, H_2O or HCO_3^-).
- Detachment (dissolution) of the product species.

For H^+ and H_2O the rate determining step will be the detachment of the product species [5], while for bicarbonate, the limiting process will be the surface co-ordination step [4]. These processes have been included in the reaction scheme by means of a simplified mechanism as a function of the rate determining step but corresponding in all cases to the overall dissolution mechanisms. Therefore, the processes included in the reaction scheme for the dissolution of the oxidised UO_2 are:

$$>UO_3 + H^+ \Rightarrow UO_2(OH)^+ \quad kH \tag{8}$$

$$>UO_3 + H_2O \Rightarrow UO_2(OH)_2(aq) \quad kH_2O \tag{9}$$

$$>UO_3 + HCO_3^- \Rightarrow UO_2CO_3(aq) + OH^- \quad kHCO_3 \tag{10}$$

$$UO_2CO_3(aq) + HCO_3^- \Rightarrow UO_2(CO_3)_2^{2-} + H^+ \quad \text{Fast} \tag{11}$$

The kinetic constants have been taken from the mechanistic models developed by de Pablo and co-workers, namely $kH = 2$ $M^{-1}s^{-1}$ [6], $kH_2O = 10^{-5}$ s^{-1} [6] and $kHCO_3 = 5 \times 10^{-2}$ $M^{-1}s^{-1}$ [4].

2.4. Other reactions in the system

The formation of $^{\cdot}OH$ radicals by decomposition of H_2O_2 has led us to introduce the recombination reactions scheme, usually used in radiolytic modelling, applied to non-irradiated UO_2 (a system without water radiolysis). In this respect, the recombination reactions lead to the regeneration of H_2O_2 and the formation of O_2, which adds to the overall oxidation of the sample under study when the oxidant is H_2O_2. Moreover, to reproduce the experiments in the presence of dissolved carbonate, the carbonate system has been also included in the reaction scheme. All these processes, the radical

recombination and the carbonate system reaction schemes, have been taken from [23].

2.5. Integration of the experimental system in the model

The dynamic dissolution experiments are reported in detail elsewhere (see [4–6]). The experimental setup consisted in a thin-film continuous flow-through reactor where powdered UO_2 was introduced and exposed to different solutions and under different oxic conditions at a constant flow rate (see Table 1). In order to reproduce the continuous flow it has been necessary to add a series of reactions simulating the transport of uranium in solution out of the system. This process can be represented by a linear, first order reaction with the kinetic constant given by the quotient between the flow rate (Q) and the volume of reaction (V):

$$\mathrm{U(VI)(aq)} \Rightarrow \mathrm{U(VI)(out)} \quad k{=}\mathrm{Q/V}\ (\mathrm{s}^{-1}) \tag{12}$$

where U(VI)(aq) represents uranium in solution. Therefore, the evolution of uranium in solution will be the balance of two processes, dissolution of the oxidised uranium (by the three mechanisms explained before) in the surface and advective transport out of the system. The output of the model will give the concentration of uranium, and when the system reaches steady state, the concentration of uranium will remain constant. From this concentration, dissolution rates can be derived using the same formula used in the experimental determination of dissolution rates (Eq. (13)):

$$R(\mathrm{mol\,m^{-2}\,s^{-1}}) = \mathrm{U(VI)(ad)} \cdot \frac{Q}{S} \tag{13}$$

where Q is the flow rate ($1\,\mathrm{s}^{-1}$), S is the total surface area (m^2) and uranium concentration is given in $\mathrm{mol\,l}^{-1}$.

Table 1
Main properties of the experimental system and conditions

Material	Powdered synthetic UO_2
Mass	1 g
Particle size	100–300 μm
BET specific area	$0.011\ \mathrm{m^2\,g^{-1}}$
Flow rate	$0.1–0.3\ \mathrm{dm^3\,day^{-1}}$
Temperature (constant)	25 °C
Experimental conditions	
Series Ia	$pO_2 = 5\%$, pH variable
Series Ib	$pO_2 = 21\%$, pH variable
Series Ic	$pO_2 = 100\%$, pH variable
Series II	pO_2 atmospheric, $[HCO_3^-]$ variable
Series III	N_2 bubbling, $[H_2O_2] = 1 \times 10^{-5}$ M, pH variable
Series IV	N_2 bubbling, $[H_2O_2]$ variable
Series V	N_2 bubbling, $[HCO_3^-] = 2 \times 10^{-3}$M, $[H_2O_2]$ variable

2.6. Assumptions and limitations of the model

The model has a number of implicit assumptions limiting its applicability. First of all, the computer code used to solve the resulting differential equations from all the kinetic reactions has been Chemsimul [24], a chemical kinetics package designed for homogeneous systems. This is one of the main limitations since we are using this code for reproducing heterogeneous systems as the solid surface/water interface is. This limitation leads to consider several approaches and assumptions:

- Surface sites and surface species must be treated as 'dissolved', simply multiplying the surface concentrations by the S/V ratio to obtain 'soluble' species.
- To achieve steady state it has been necessary to impose that the concentration of the species $>UO_3$, representing oxidised sites, must be much lower than the concentration of the species $>UO_2$, the reactive sites (low pre-oxidation or passivation).

Further work is underway to try to overcome these limitations.

3. Results and discussion

3.1. Calibration of the oxygen promoted mechanism

The results of applying the model to the experiments in series I are shown in Fig. 1. As already discussed in [3], experimental results indicate that between pH 3 and 6.5, approximately, the dissolution rate decreases with increasing pH, and it increases with higher oxygen concentration. Dissolution rates for pH values higher than 6.5 are relatively low, not dependent on pH, and similar for all O_2 concentrations. The dependence of the dissolution rates on the oxygen concentration is reproduced by the model and in agreement with the mechanism developed by de Pablo et al. [6].

In the acidic range, the surface co-ordination with H^+ is the rate determining step and consequently there is a linear dependence of the dissolution rate on the proton concentration. In the neutral range, the surface co-ordination by water will be the rate determining step with no dependence on pH. Both pH ranges in the 5% and 21% O_2 experiments are well reproduced by the model presented in this work and in agreement with the model developed by de Pablo et al. [6]. Differences can be due to the uncertainty in determining the reactive volume, the thin effective layer where the powdered UO_2 is located in the column.

In the alkaline range, we might expect an increase of the dissolution rate when increasing the pH of the system given by the surface complexation by the hydroxyl anion as the rate-determining step. However,

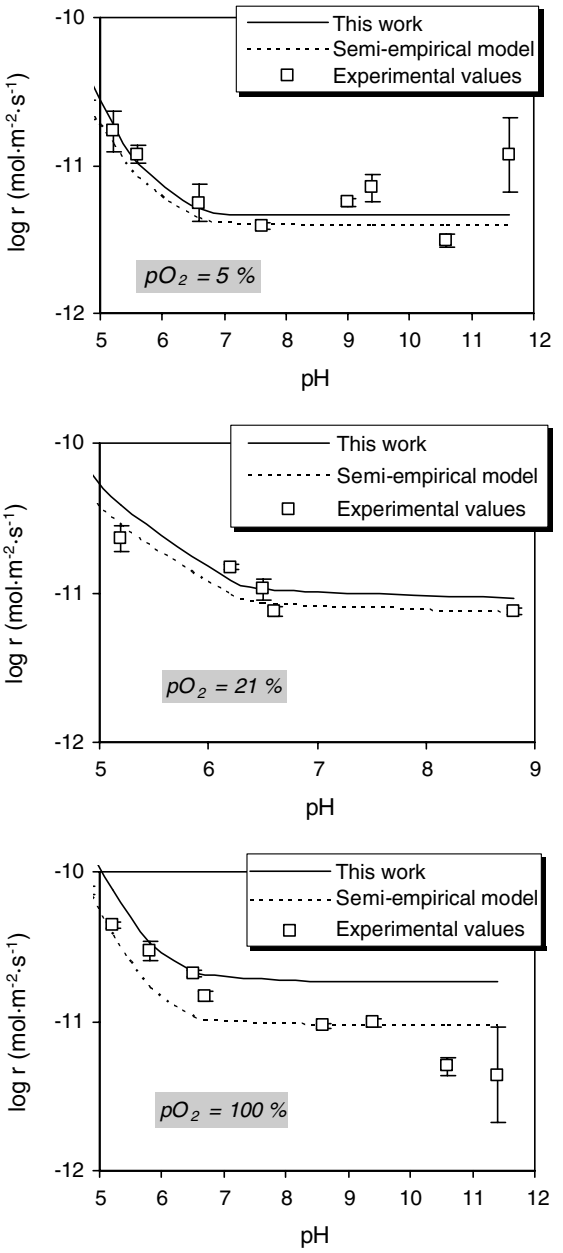

Fig. 1. Results of the model applied to series I experiments compared to experimental values [3] and semi-empirical model [6].

experimental data indicates no dependence with pH in the alkaline range. In addition, there is no rate increase with increased oxygen content of the system. This behaviour might be interpreted as being caused by the precipitation of a secondary phase, probably a Na-uranate as $NaClO_4$ was present to control ionic strength in this system. In Fig. 2 we can see the good fitting of the uranium dissolution data when considering equilibrium

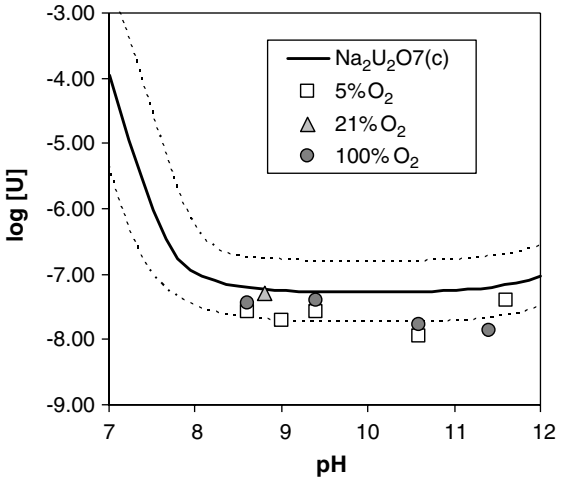

Fig. 2. Solubility curve of $Na_2U_2O_7$ (log K_s from [27]) and uranium concentrations measured at the steady-state in the different experimental tests (data taken from [3]).

with $Na_2U_2O_7$ (other phases could be involved, such as Na-polyuranates, but the one selected here produced the best fit). The high stability of these phases at alkaline conditions and the fast kinetics of precipitation of these compounds (Bruno, pers. comm.) make the formation of a precipitate a hypothesis that cannot be ruled out taking into account that the residence time of the solution in the reactor is approximately 1 h. Thomas and Till [28] also interpreted the decrease of their dissolution rates at high temperatures in the alkaline range by passivation effects due to the deposition of some uranyl phase such as $NaUO_3$ or $Na_2U_2O_7$. The precipitation process is also supported by the fact that XPS analysis after the leaching experiments found an oxidised surface at all O_2 concentrations and alkaline pH [3].

The calibration process of our model has led to a good fit for pH > 5, and for oxygen partial pressures of 0.05 and 0.21 bar, which therefore represent the range of applicability of our model.

The next series of experiments, series II, was modelled by adding the carbonate system in the reaction scheme and running several simulations with different HCO_3^- concentrations in the system. Experimental results (Fig. 3) show a linear dependence of dissolution rate with respect to bicarbonate concentration until approximately $[HCO_3^-] = 10^{-2}$ M, where it becomes independent of $[HCO_3^-]$. This feature was already reproduced in [4], and it was attributed to the sorption of oxygen on the surface of the solid being the rate determining step, slower than both bicarbonate attack and detachment of the complex formed. We have not been able to reproduce this behaviour at high HCO_3^- content, most probably due to a lack of a mechanism accounting for the saturation of oxidised sites. On the other hand, at

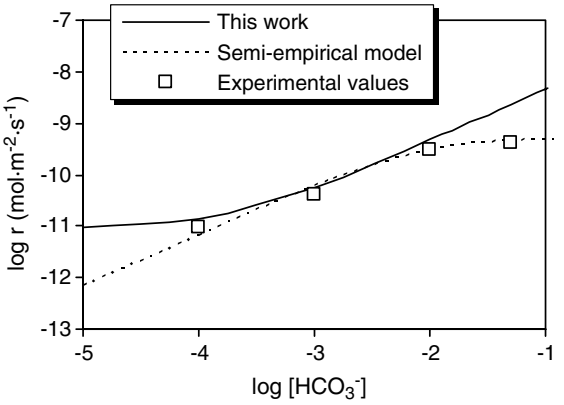

Fig. 3. Results of the model applied to series II experiments compared to experimental values and semi-empirical model described in [4].

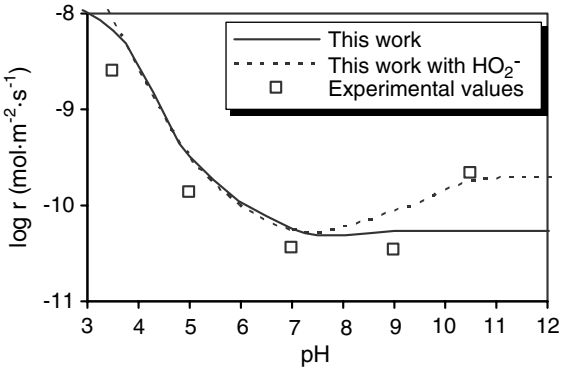

Fig. 4. Results of the model applied to series III experiments compared to experimental values described in [5].

low carbonate content our model gives a constant dissolution rate due to the inclusion of protonation and water molecule complexation, the predominant processes under very low carbonate content. These processes are not included in [4] and this is the reason why both models diverge in this carbonate range.

According to the previous discussion, the model at present is capable to reproduce experimental data for $[HCO_3^-] < 10^{-2}$ M. Further work is necessary in order to include saturation effects in the kinetic scheme.

It must be noted that the mechanistic models developed by de Pablo et al. [4,6,11] were different for the two separate series of experiments (series Ia, Ib and Ic with varying oxygen content, carbonate free; and series II with varying amount of carbonate). Our model has been able to reproduce both series with a unique set of reactions and kinetic constants, representing a unified conceptual and numerical approach to the kinetic modelling of this type of experiments.

3.2. Calibration of the H_2O_2 promoted mechanism

The application of our model to the experiments with H_2O_2 (series III, IV and V in Table 1) is explained in the following paragraphs. As stated earlier, it should be pointed out that decomposition of H_2O_2 leads to the formation of O_2 through the radical recombination mechanism, adding to the overall oxidation of the UO_2.

As it can be seen from experimental values (Fig. 4) the dissolution rate decreases with pH in the acidic range and increases at alkaline pH. The decreasing trend at low pH is correctly predicted by our model, although the line lies above the experimental values. Again, this discrepancy may be due to the uncertainty in the determining the reactive volume.

At alkaline conditions the model predicts a constant dissolution rate (solid line in Fig. 4), as was the case for the experiments with O_2, this is mainly due to the fact previously noticed that the uranium dissolution mechanism only takes into account the complexation with the H^+ and the water molecule. This contrasts with the experimental evidence of a higher dissolution rate at high pH. As de Pablo et al. [5] pointed out, this higher dissolution rate is probably due to the decomposition of H_2O_2 into HO_2^- ($pKa = 11.6$), a more reactive species able to form strong complexes with the uranyl cation not included in our oxidative dissolution mechanism. The uranyl-mono-hydrogenperoxo species has been described in uranyl solutions with H_2O_2 at pH < 6 [25]. Complexation of other metal species like Fe(III) and Tl(III) with hydrogen peroxide have been also studied leading to mono- and di-(hydrogenperoxo)M(III) species in H_2O_2 [29,30]. Some authors also highlight that hydrogen peroxide may also form complexes with coordination sites slightly basic (alkaline range) leading to higher dissolution rates [31]. In order to test the capability of our model, we have run a simulation with a new process whereby oxidised uranium at the surface can be complexed by the perhydroxy anion. At alkaline conditions a negatively charged complex formed through hydrolysis should be expected according to the following reaction:

$$UO_2^{2+} + 3HO_2^- = UO_2(HO_2)_3^- \quad (14)$$

A simplified mechanism representing this process has been included in the reaction scheme. The result of this exercise is also shown in Fig. 4 (dotted line). In such case, the higher dissolution rate in the alkaline range is reproduced by the model. Other processes could be postulated to explain the observed phenomenon of higher dissolution rates at alkaline pH, and further work is underway to try to elucidate this issue.

For the experiments with varying concentrations of H_2O_2 (series IV, Fig. 5), dissolution rates increased with H_2O_2 concentration until 10^{-4} M, where a plateau was reached. The model developed by de Pablo et al. [5],

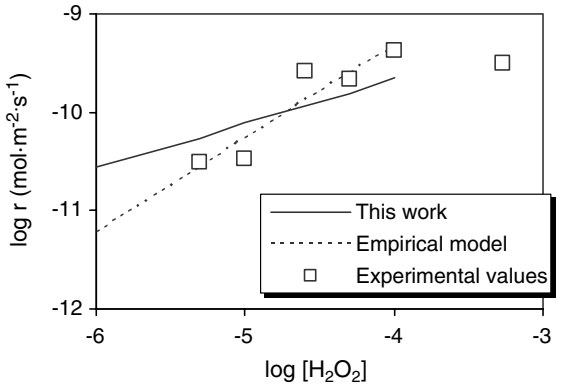

Fig. 5. Results of the model applied to series IV experiments compared to experimental values and empirical model (regression analysis) described in [5].

namely a regression analysis for the points with $H_2O_2 < 10^{-4}$ M, gave a reaction order close to one. Interestingly, our model also reproduces the experimental data with reasonable agreement, but it gives a slope lower than 1. This indicates a fractional order as a result of surface mediated kinetics and the consequent parallel reactions taking place in the system. In other words, the main oxidising species, the $^{\cdot}OH$ radical produced in the surface decomposition of H_2O_2, is consumed not only by UO_2, but also by other species in the recombination reactions. On the other hand, we have not tried to fit the data points with H_2O_2 concentrations higher than 10^{-4} M, as it has been experimentally shown that dissolution rates are independent of H_2O_2 at high concentrations [5,26].

The last experiments included in this work are the flow-through experiments performed at different concentrations of H_2O_2 and a constant concentration of bicarbonate, 2×10^{-3} M (series V, Fig. 6). Measured dissolution rates were higher than in the absence of bicarbonate, and they also showed a plateau at high H_2O_2 concentrations. The regression analysis carried out by de Pablo et al. [5] gave a fractional order, as well as our model although with a slightly lower slope. Nonetheless, both models show a fairly good fit to the experimental data. Previous attempts to apply our model to these experiments without the decomposition of H_2O_2 in hydroxyl radicals failed as there was no mechanism of interaction between hydrogen peroxide and carbonate. As stated in the conceptual and mathematical model section, our model takes into account all the reactions of the carbonate system, including a reaction between $^{\cdot}OH$ and HCO_3^-. It appears that this simple reaction is essential to explain the behaviour of the system. Moreover, the corresponding kinetic constant of the reaction between $^{\cdot}OH$ and HCO_3^- has been taken from the literature, without the need of further calibration. It should be pointed out, however, that until now only experiments with $[HCO_3^-] = 2 \times 10^{-3}$ M have been included in this modelling exercise, and further work is underway to include a series of experiments with varying content of carbonate.

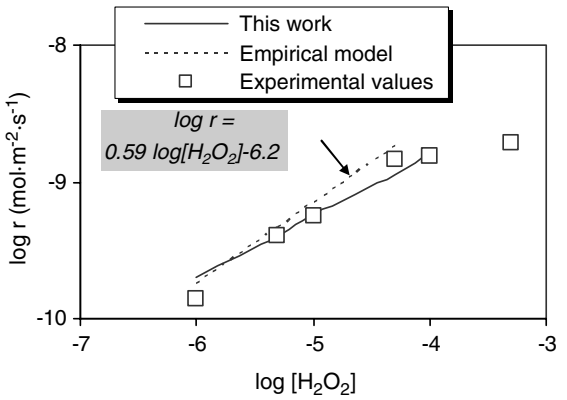

Fig. 6. Results of the model applied to series V experiments compared to experimental values and empirical model (regression analysis) described in [5].

4. Conclusions

Flow-through dissolution experiments with unirradiated UO_2 have been used to calibrate the oxidative dissolution mechanism of UO_2. The model developed has been able to reproduce experimental dissolution rates for pH > 5 and $[HCO_3^-] < 10^{-2}$ M when the oxidant is O_2 at partial pressures lower than 21%, and $3 <$ pH < 9 and $[HCO_3^-] = 2 \times 10^{-3}$ M when the oxidant is H_2O_2 at concentrations below 10^{-4} M. Moreover, the calibration process has provided some insight into the detailed mechanism taking place in the alteration of UO_2 in the presence of water. In particular, the simplified mechanism of UO_2 oxidation by H_2O_2 involving hydroxyl radicals has been useful in reproducing the observed interaction between H_2O_2 and carbonate present in the leachant. The results show that, although more simulations are needed, the calibrated oxidative dissolution mechanism could be included in radiolytic models to gain confidence in the prediction of the long-term alteration rate of the spent fuel under repository conditions, which is our ultimate goal.

Acknowledgements

Financial support for this research has been provided by ENRESA (Empresa Nacional de Residuos Radiactivos) and in the framework of the European Commission project SFS (Spent Fuel Stability), Contract No. FIKW-CT-2001-20192.

References

[1] C. Poinssot, M. Cowper, B. Grambow, J.M. Cavedon, T. McMenamin, in: EURADWASTE '04, 29–31 March 2004, Luxembourg. Available from: <http://www.cordis.lu/fp6-euratom/ev_euradwaste04.htm>.

[2] J. Merino, E. Cera, J. Bruno, in: Proceedings of the Workshop on Modelling the Behaviour of Spent Fuel under Repository Conditions, 5–7 June 2002, Ávila, Spain, CIEMAT, Serie Ponencias.

[3] M.E. Torrero, E. Baraj, J. de Pablo, J. Giménez, I. Casas, Int. J. Chem. Kinet. 29 (1997) 261.

[4] J. de Pablo, I. Casas, J. Giménez, M. Molera, M. Rovira, L. Duro, J. Bruno, Geochim. Cosmochim Acta 63 (19/20) (1999) 3097.

[5] J. de Pablo, I. Casas, F. Clarens, J. Giménez, M. Rovira, Contribución experimental y modelización de procesos básicos para el desarrollo del modelo de alteración de la matriz del combustible irradiado. Publicación Técnica Enresa 01/2003.

[6] J. de Pablo, I. Casas, J. Giménez, F. Clarens, L. Duro, J. Bruno, Mat. Res. Soc. Symp. Proc. 807 (2004) 83.

[7] J. Bruno, E. Cera, L. Duro, J. Pon, J. de Pablo, T.E. Eriksen, Application of the model to the minor radionuclides, SKB Technical Report 98-22, 1998.

[8] J. Quiñones, J. serrano, P. Díaz Arocas, J.L. Rodríguez Almazán, J. Bruno, E. Cera, J. Merino, J.A. Esteban, A. Martínez-Esparza, Cálculo de la generación de productos radiolíticos en agua por radiación a. Determinación de la velocidad de alteración de la matriz del combustible nuclear gastado, ENRESA Publicación Técnica 02/00, 2000.

[9] E. Cera, J. Merino, J. Bruno, Liberación de los radionucleidos e isótopos estables contenidos en la matriz del combustible. Modelo conceptual y matemático del comportamiento del residuo, ENRESA Publicación Técnica 03/00, 2000.

[10] J. Merino, E. Cera, J. Bruno, T. Eriksen, J. Quiñones, A. Martínez-Esparza, in: ICEM'01, The 8th International Conference on Radioactive Waste Management and Environmental Remediation, September 30–October 4 2001, Bruges (Brugge), Belgium.

[11] W.E. Schortmann, M.A. DeSesa, in: 2nd United Nations International Conference on the Peaceful Uses of Atomic Energy, Geneva, 1958, Proceedings, Vol. 3, p. 333.

[12] D.W. Shoesmith, J. Nucl. Mater. 282 (2000) 1.

[13] J. Giménez, F. Clarens, I. Casas, M. Rovira, J. de Pablo, J. Bruno, J. Nucl. Mater. 345 (2005) 232.

[14] F. Clarens, J. de Pablo, I. Casas, J. Giménez, M. Rovira, Mat. Res. Soc. Symp. Proc. 807 (2004) 71.

[15] J.O. Edwards, R. Curci, in: G. Strukul (Ed.), Catalytic Oxidations with Hydrogen Peroxide as Oxidant, Kluwer Academic, Dordrecht, 1992, p. 111.

[16] R. Andreozzi, V. Caprio, A. Insola, R. Marotta, Catal. Today 53 (1999) 51.

[17] L.A. Salem, R.I. Elhag, M.S. Khalil, Trans. Metal Chem. 25 (3) (2000) 260.

[18] J. Abbot, D.G. Brown, Int. J. Chem. Kinet. 22 (1990) 963.

[19] J. de Pablo, I. Casas, F. Clarens, F. El Aamrani, M. Rovira, Mater. Res. Soc. Symp. Proc. 663 (2001) 409.

[20] J. Bruno, E. Cera, T.E. Eriksen, M. Grivé, S. Ripoll, Mat. Res. Soc. Symp. Proc. 807 (2004) 397.

[21] E. Ekeroth, M. Jonsson, J. Nucl. Mater. 322 (2003) 242.

[22] C.M. Miller, R.L. Valentine, Water Res. 33 (12) (1999) 2805.

[23] M. Kelm, E. Bohnert, FzK report FZKA 6977, 2004.

[24] P. Kirkegaard, E. Bjergbakke, CHEMSIMUL: a simulator for chemical kinetics. Roskilde, Denmark: Riso National Laboratory, Riso-R-1085(EN), 2002.

[25] R. Djogic, B. Raspor, M. Branica, Croatica Chemica Acta 66 (2) (1993) 363.

[26] D.W. Shoesmith, S. Sunder, J. Nucl. Mater. 190 (1992) 20.

[27] I. Grenthe, J. Fuger, R.J.M. Konings, R.J. Lemire, A.B. Muller, C. Nguyen-Trung, H. Wanner, Chemical Thermodynamics, in: Wanner, Forest (Eds.), Chemical Thermodynamics of Uranium. NEA-OECD, Vol. 1, Elsevier, 1992.

[28] G.F. Thomas, G. Till, Nucl. Chem. Waste Manage. 5 (1984) 141.

[29] Z. Boti, I. Horvath, Z. Szil, L.J. Csanyl, J. Chem. Soc., Dalton Trans.: Inorg. Chem. (1972–1999) 9 (1978) 1012.

[30] H. Gallard, J. De Laat, B. Legubeb, Water Res. 33 (13) (1999) 2929.

[31] S.S. Chou, C.P. Huang, Appl. Catal. A: Gen. 185 (2) (1999) 237.